

## Application of Micromachining in the PLC Optical Splitter Packaging

Byoung-Chan Choi\* and Man-Seop Lee

*ICU Optical Network and Systems Laboratory, Daejeon 305-732, KOREA*

Ji-Hoon Choi and Chan-Sik Park

*Phoco. Co. Ltd.*

*ICU TBI Center 32222, Daejeon 305-732, KOREA*

(Received June 27, 2003)

This paper presents micromachining results on planar-lightwave-circuit (PLC) chips with Si substrate and the quartz substrate by using Ti:Sapphire femtosecond-pulsed laser. The ablation process with femtosecond laser pulses generates nothing of contamination, molten zone, microcracks, shock wave, delamination and recast layer. We also showed that the micromachine for PLC using femtosecond pulsed lasers is superior to that using nanosecond pulsed lasers. The insertion loss and the optical return loss of the  $1 \times 8$  optical power splitters packaged with micromachined input- and output-port U-grooves were less than 11.0 dB and more than 55 dB, respectively. The wavelength dependent loss (WDL) was distributed within  $\pm 0.6$  dB and the polarization dependent loss (PDL) was less than 0.2 dB.

*OCIS codes* : 140.3390, 140.3330, 230.1150, 160.4760.

### I. INTRODUCTION

Lasers have been used successfully for the micromachining of metals, ceramic, plastic and other materials. There are a number of advantages in using lasers for micromachining: single-step processing; high flexibility; direct writing of structures by moving the laser beam at speeds much faster than speeds obtained with mechanical tools; no contamination of the material being processed; sterility which is important for medical and biological applications, and the precise focusing of beam spot size which makes possible to lead a highly localized treatment of materials with a spatial resolution better than  $1 \mu\text{m}$ . However, with many materials, this high spatial resolution normally cannot be achieved using standard nanosecond lasers due to strong thermal effects. The thermal effects occur in the material and the destructive influence of the plasma that is formed above the surface. There are two main ways of minimizing these destructive effects when structures with dimensions on the order of micrometers are required. Ultraviolet (UV) laser lights can be used since UV laser lights can, in principle, be focused on to smaller areas. Moreover, since materials generally have a much higher absorption in the UV light, concentrating the absorbed energy in a relatively

small area leads to controllable material removal. But we should keep in mind that excimer lasers, which are the most typical UV lasers, usually have relatively poor beam qualities. UV lasers also cause non-thermal excitations and photochemical bond breaking, which are more important in micromachining applications of UV lasers. This approach has led to a reasonable damage suppression in structures on the order of  $10 \sim 100 \mu\text{m}$  dimensions or less for many materials such as polymers [1], biological tissue [2] and some ceramic materials [3]. The accuracy and reproducibility are, however, still limited. The other approach to minimizing the destructive effects is to use femtosecond laser pulses [4–11]. In addition to reducing the destructive thermal effects due to the much shorter time scale for the energy coupling into the material and eliminating the laser-plasma interaction above the surface, the use of femtosecond laser pulses can induce the multiphoton absorption and the non-linear optical effects. The former leads to a much smaller absorption volume than that of single-photon absorption which can give a much more controllable removal of material and also serves to reduce further the thermal stress in the bulk material. One of the non-linear optical effects is self-focusing of the laser beam in the transparent material due to the optical Kerr effects. Under cer-

tain conditions, this self-focusing effect can be manipulated to produce precise microstructures. Therefore femtosecond-pulsed laser micromachining techniques can be also applied to precise machining applications with sub-micrometer feature sizes such as jet printer nozzles, micro-optical devices and arrays, MEMS devices, bio-chips, semiconductor devices and related devices [1–11].

Silica glass ( $\text{SiO}_2$ ) is one of the most important materials in the fields of optoelectronics, micro-optics and fiber technology [12]. It has a high transmission from the UV to infrared (IR) wavelength, excellent thermal and electrical properties and high chemical resistivity. These properties also make it a particularly challenging material for micromachining applications. In this paper we will show that it is possible to ablate highly reproducible U-grooves on PLC chips, which are useful for applications in optical devices, by using an 800 nm laser beam from a commercial Ti:sapphire femtosecond-pulsed laser. Machining results of the femtosecond-pulsed laser are compared with those of nanosecond-pulsed laser with wavelengths in the ultraviolet range. We will also demonstrate optical properties of packaged PLC splitters using the grooved chips.

## II. THEORETICAL BACKGROUND

Ablation with femtosecond laser pulses takes place as follows process: At first, the laser radiation is absorbed inside the surface layer by bound electrons and free electrons. This is accompanied with the excitation and ionization of the material and heating of free electrons by inverse bremsstrahlung. At this process, the absorbed laser energy is deposited into the electronic subsystem.

The rapid absorption process is followed by an energy transfer from the electron to the lattice (atomic subsystem), bond breaking, and material expansion. The thermal diffusion into the material is usually negligible because these processes happen on a picosecond time scale for laser fluence close to the ablation threshold. Therefore, the ablation occurs without the formation of heat- and shock-affected zones.

During the interaction of low energy density femtosecond laser pulses, the laser energy is mainly absorbed by free electrons due to the inverse bremsstrahlung. The absorption process is followed by fast energy relaxation within the electron subsystem. The energy relaxation accompanies the energy transfer from the electrons to the lattice and the heat transport into the material due to the electron thermal diffusion. Assuming that the thermalization within the electron subsystem is very fast and that the electron and the lattice subsystems can be characterized by electron temperature  $T_e$  and lattice temperature

$T_i$ , laser-material energy interaction can be described by the following one-dimensional two-temperature diffusion model [4,5]:

$$C_e \frac{\partial T_e}{\partial t} = -\frac{\partial Q(z)}{\partial z} - \gamma(T_e - T_i) + S \quad (1)$$

$$C_i \frac{\partial T_i}{\partial t} = \gamma(T_e - T_i) \quad (2)$$

where  $z$  is the direction perpendicular to the material surface, and  $Q(z) = -k_e \partial T_e / \partial z$  is the electron heat flux (the thermal conductivity of the lattice subsystem is neglected) for the electron thermal conductivity  $k_e$ .  $S = I(t)A\alpha \exp(-\alpha z)$  is the laser heating source term, where  $I(t)$  is the laser intensity,  $A$  is the surface transmissivity ( $A = 1 - R$  where  $R$  is reflectivity at material surface) and  $\alpha$  is the material absorption coefficient.  $C_e$  and  $C_i$  are the heat capacities per unit volume of the electron and the lattice subsystem with  $C_e = C'_e T_e$  (where  $C'_e$  is constant), respectively.  $\gamma$  represents the electron-lattice coupling.

We define the electron cooling time (in the order of 1 ps) as  $\tau_e = \frac{C_e}{\gamma}$ , the lattice heating time (some 100 ps) as  $\tau_i = \frac{C_i}{\gamma}$  and the pulse duration as  $\tau_H$ , then we can analyze Eqs. (1) and (2) into three characteristic time scales (due to the electron-lattice coupling):

$$\tau_H \leq \tau_e, \tau_i \quad (3)$$

$$\tau_H \leq \tau_i \quad (4)$$

$$\tau_e, \tau_i \leq \tau_H \quad (5)$$

The time regime of Eq. (3) includes the pulse duration of the femtosecond laser. A more detailed comparison with other regimes is given in [4–7].

When  $\tau_H \ll \tau_e, \tau_i$ , the electron-lattice coupling can be neglected during the laser pulse. In this case Eqs. (1) and (2) can be easily solved. The general solution of this equation is quite complicated. We can simplify the equation by neglecting the heat-flux term of electrons,  $Q(z) = -k_e \partial T_e / \partial z$ , in Eq. (1). This condition can be satisfied when  $D_e \tau_H < \alpha^{-2}$ , where  $D_e = k_e / C_e$  is defined as the electron thermal diffusivity. In this case Eqs. (1) and (2) can be solved:

$$T_e(t) = \left[ T_0^2 + \frac{2I_0 A \alpha}{C'_e} t \exp(-\alpha z) \right]^{1/2} \quad (6)$$

Here  $I(t) = I_0$  is assumed to be constant,  $T_e(0) = T_0$  is the initial temperature. At the end of the laser pulse the electron temperature comes to  $T_e(\tau_H) \gg T_0$ , then Eq. (6) can be simplified as

$$T_e(\tau_H) \approx \left( \frac{2F_a \alpha}{C'_e} \right)^{1/2} \exp\left(-\frac{\alpha z}{2}\right) \quad (7)$$

where  $F_a = I_0 A \tau_H$  is the absorbed laser fluence.

Eqs. (1) and (2) describes the evolution of the electron and lattice temperature with  $S = 0$  after the laser pulse strikes on the material surface. Initial conditions are given by Eq. (7) and  $T_i = T_0$ . After the laser pulse strikes, the electrons are rapidly cooled due to the energy transfer to the lattice and the heat conduction into the bulk. Since the cooling time of the electron subsystem is very short, Eq. (2) can be written as  $T_i \approx T_e(\tau_H)t/\tau_i$  (here the initial lattice temperature is neglected). The attainable lattice temperature is determined by the average cooling time of the electron  $\tau_e^a = C_e' T_e(\tau_H)/2\gamma$  and can therefore be written as

$$T_i(\tau_e^a) \approx T_e^2 \frac{C_e'}{2C_i} \approx \frac{F_a \alpha}{C_i} \exp(-\alpha z) \quad (8)$$

The evaporation kinetics can be described by the Arrhenius-type equation [13]

$$V = V_0 \exp\left(-\frac{\rho\Omega}{C_i T_i}\right) \quad (9)$$

where  $\rho$  is the density,  $\Omega$  is the specific heat of evaporation (per unit mass),  $V$  is the velocity of the evaporation front and  $V_0$  is a constant depending on the material (of the order of the sound velocity in the condensed phase). Using Eq. (8), the laser fluence is represented by

$$F_a \approx \frac{T_i(\tau_e^a) C_i}{\alpha} \exp(\alpha z) \quad (10)$$

Significant evaporation occurs when  $C_i T_i$  becomes larger than  $\rho\Omega$ , then the laser fluence is obtained by

$$F_a \geq F_{th} \exp(\alpha z) \quad (11)$$

where  $F_{th} \cong \rho\Omega/\alpha$  is the threshold laser fluence for evaporation with femtosecond laser pulses.

### III. EXPERIMENTAL

#### 1. Specimen

Silica-based PLC splitter is a key component in optical access networks such as passive optical networks (PON). Specimens of PLC splitter chips used in the experiment were the ones fabricated on a quartz substrate with conventional PLC technology using flame hydrolysis deposition (FHD) and reactive ion etching (RIE) techniques [12,14]. The basic size of the rectangular core is  $8 \times 8 \mu\text{m}$  and the refractive index difference between the core and the cladding is about 0.3%. The sample dimension is  $4.5 \text{ mm} \times 30 \text{ mm} \times 1.048 \text{ mm}$ .

#### 2. Laser System and Machining Experiment

The nanosecond ablation experiments were performed using a KrF excimer laser system with a repetition rate of 200 Hz and pulse energy of 30 mJ at  $\lambda = 248 \text{ nm}$  and an ArF excimer laser system with 100 Hz-repetition rate and 42 mJ-pulse energy at  $\lambda = 193 \text{ nm}$ . Both excimer laser systems have the pulse duration of 20 to 30 ns. Laser pulses were uniformly illuminated onto samples using a circular aperture of  $< 100 \mu\text{m}$  diameter and a 10 cm focal-length lens.

The femtosecond ablation experiments were performed using a Ti:Sapphire laser system, consisting of a Ti:sapphire oscillator and an amplifier system based on the chirped pulse amplification was used for the ablation with the pulse duration of 100 fs, the repetition rate of 1 kHz and the pulse energy of 1 mJ at  $\lambda = 800 \text{ nm}$ . The laser pulses are focused with a 30 mm focal-length quartz lens giving an spot size of  $6 \mu\text{m}$  at the sample. The spatial profile of the laser pulse is nearly Gaussian. The fluence (energy per unit area) varies over the spatial profile of the laser beam. The fluence is controlled by changing the total incident energy with a half-wave plate and a polarizer. The polarization of the laser pulse is controlled by a second half-wave plate. Fig. 1 shows the schematic of the femtosecond-pulsed laser system.

The samples were mounted on computer-controlled X-Y-Z- $\Theta$  translation stages such that the laser processed-area was free-standing. We translated the sample by approximately  $1 \mu\text{m}$  between runs. The position, size and center of the optical waveguide on the PLC chip were measured by a vision system. The experiments were carried out in air. We formed U-grooves in one-input and 8-output port on the PLC splitter chip. The U-groove size is  $126 \mu\text{m} \times 87 \mu\text{m} \times 2 \text{ mm}$  and the allowable margin of error was controlled within  $\pm 1 \mu\text{m}$ . Fig. 2 represents a schematic of machined U-grooves on the PLC chip.

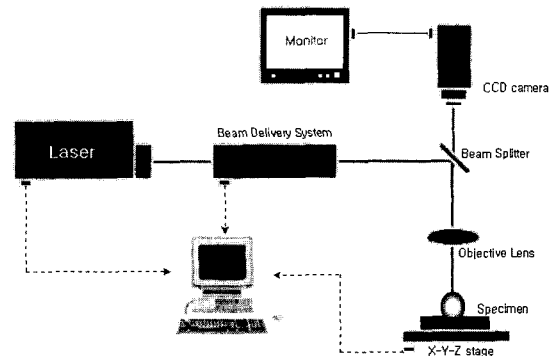


FIG. 1. A schematic of femtosecond-pulsed laser system

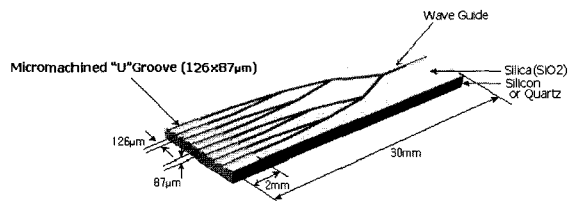


FIG. 2. A schematic of machined U-groove on the PLC chip

#### IV. RESULT AND DISCUSSION

##### 1. Machining Results and Discussion

###### A. Silica-based waveguides on the Si substrate

With the excimer laser based on nanosecond pulse duration, the heat transferred from the laser beam to the work piece introduced a lot of restrictions that limit the precision and the quality of the machining process as shown in Figs. 3 and 4 analyzed with op-

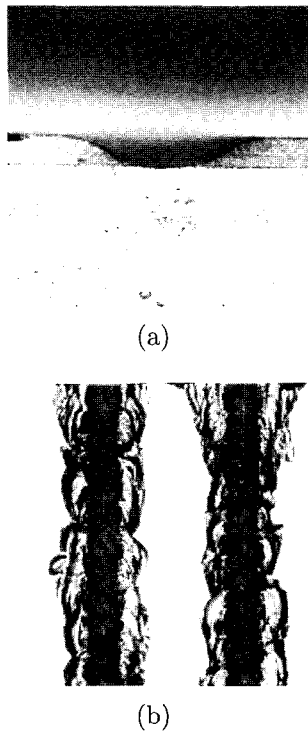
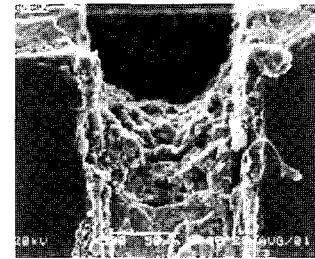
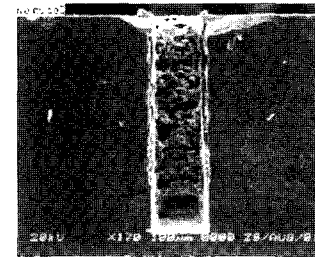


FIG. 3. U-grooves on PLC chip based on the Si substrate, machined by using 248 nm KrF excimer laser with nanosecond pulse duration (300 Hz, 20 mJ): (a) side view( $\times 500$ ) and (b) top view( $\times 200$ ).



(a)



(b)

FIG. 4. U-grooves on PLC chip based on the Si substrate, machined by using 193 nm excimer laser with nanosecond pulse duration (100 Hz, 42 mJ): (a) side view( $\times 500$ ) and (b) top view( $\times 170$ ).

tical microscope (OM) and scanning electron microscope (SEM). A large amount of debris is created during the machining process. The debris, whose form depends on the material being machined, can be very difficult to remove. A large heat-affected zone (HAZ) completely surrounds the U-groove channel. A heavy recast layer is immediately presented along both edges of the U-groove. Outside the recast layer, an extended zone of debris (droplets of molten  $\text{SiO}_2$ ) is visible. This debris was still extremely hot when it landed on the surface. Removing this material will require substantial post processing efforts, if it can be done at all without damaging the surface. Shock waves also are observed near both U-groove edges as shown in Fig. 3(b). In particular, we could not make the U-groove shape with desirable dimension of  $126 \mu\text{m} \times 87 \mu\text{m} \times 2 \text{mm}$  using the excimer laser. The situation is quite different when working with femtosecond lasers.

Fig. 5 shows machined results by femtosecond laser pulses in a PLC chip, which has the silica-based waveguide on the Si substrate. It is quite obvious that the U-grooves machined with femtosecond laser pulses are cleaner than those machined with nanosecond laser pulses. The open to air condition of the micromachining process was under theoretical limitation for femtosecond laser pulses. In case of the PLC chips with multi-layers, which are formed transparent material on the Si substrate, however, laser ablation initially occurred at interface between layers. This phenomenon is due to the different laser absorption

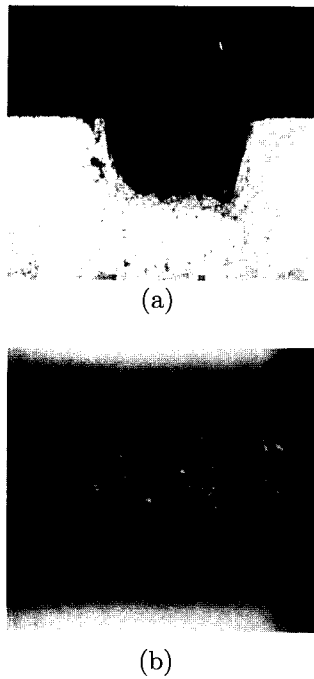


FIG. 5. U-grooves on PLC chip based on the Si substrate, machined by Ti:Sapphire laser with femtosecond pulse duration (1 kHz, 1 mJ): (a) side view( $\times 500$ ) and (b) top view( $\times 500$ ) at bottom surface of U-groove.

and the different ablation threshold of the materials. Another likely reason may be that typical air condition deteriorate the machining quality because of the

air breakdown phenomenon due to air-ionization. So it is difficult to obtain a desirable dimension of the U-groove. We also could not reduce the roughness of the bottom surface to be less than  $10 \mu\text{m}$  in the PLC chip because of stacks of molten materials as shown in Fig. 5.

Note that one could improve the surface roughness of the micromachining process by using other types of air jets such as  $\text{N}_2$  gas and Ar gas [11]. The air jet would be able to physically blow molten phase materials away from the work zone.

*B. Silica-based waveguides on the quartz substrate*

It was reported that recast layers, broken edges, shock waves, and HAZ were visible in the quartz materials and the silica glasses during micromachining those materials by the excimer laser with nanosecond pulse duration [9,16]. In our experiments, silica glass materials were used as specimens. When the excimer laser based on nanosecond pulses is initially illuminated at the surface of PLC splitter chip, further improvements were not observed and the features of micromachining were almost same as shown in Figs. 3 and 4. Therefore it would be reasonable to conclude that nanosecond laser pulses cannot make a desirable U-groove in the PLC chips, which has the silica-based waveguide on the quartz substrate.

To improve roughness of silica-based waveguide on

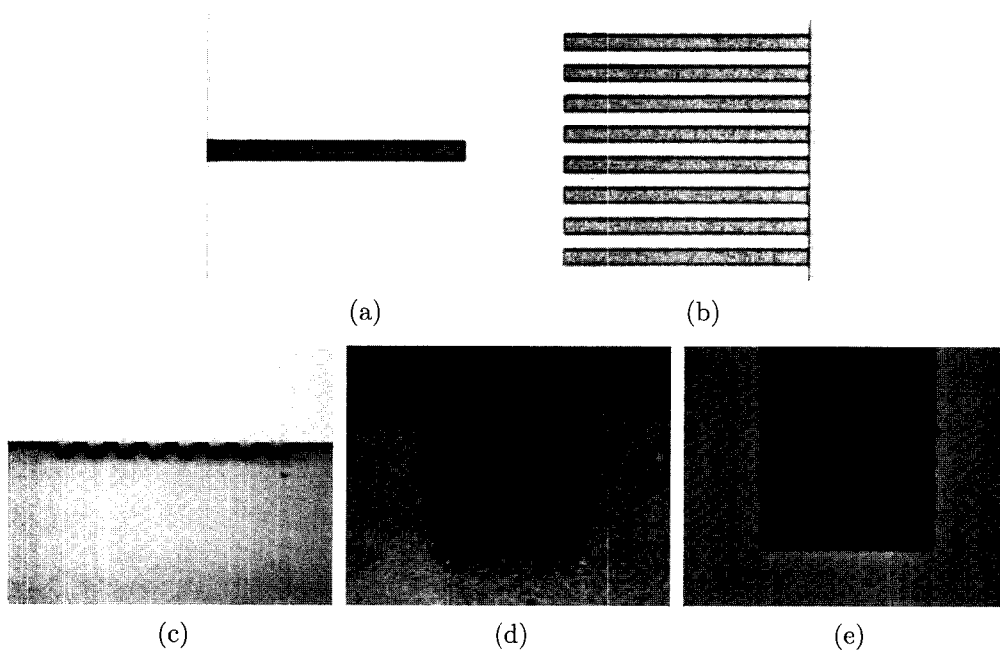


FIG. 6. Machined U-grooves of one-input and 8-output channel analyzed with the optical microscope; (a) one input port( $\times 50$ ), (b) and (c) 8 output ports( $\times 50$ ), (d) and (e) one port magnified( $\times 500$ ).

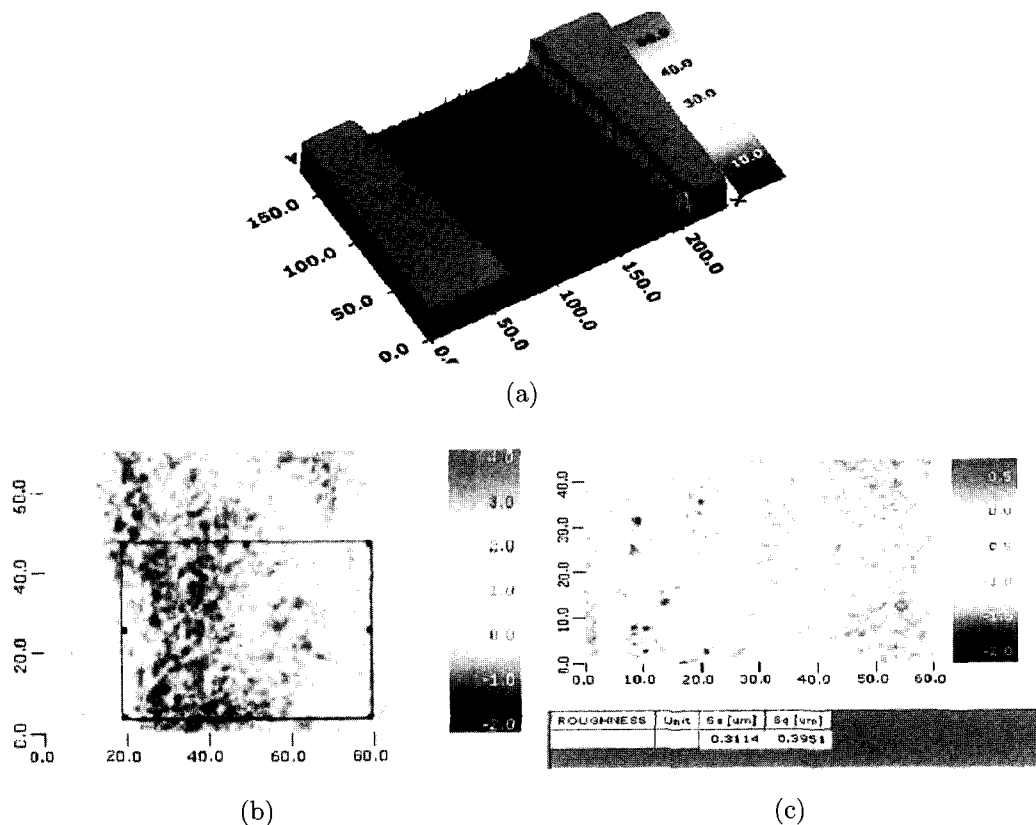


FIG. 7. 3D profiles of U-groove analyzed with a 3D Surface Profiling System; (a) overall view ( $\times 20$ ), (b) roughness bottom ( $\times 50$ ), (c) roughness of bottom zoomed the rectangular region of (b) ( $\times 50$ ).

quartz substrate, we tried to machine the U-grooves in the PLC chips with a femtosecond-pulsed Ti:sapphire laser: The waveguide layer and substrate of PLC chips are the same material. We also used a dry air jet during machining process to remove the melted phase material away from the work zone. It is quite obvious that the U-grooves, machined with femtosecond laser pulses, are very clean as shown in Fig. 6. Note also very limited HAZ and the absence of recast layer. The edges of the U-groove are straighter and sharper than those of Fig. 4. Overall the quality of the machining is much better than those of the excimer laser micromachining. The U-groove size of each waveguide of  $1 \times 8$  PLC optical splitter is  $126 \mu\text{m}$ -width,  $87 \mu\text{m}$ -depth, and  $2 \text{ mm}$ -length within tolerance of  $\pm 1 \mu\text{m}$ .

The main feature of laser-material interaction in the femtosecond laser pulses is that the heat deposited onto the material by the laser does not have time to move away from the work spot during the induced time of the laser pulse. The reason for no heat diffusion is due to the duration of the laser pulse shorter than the heat diffusion time [4–11]. Because the energy does not have the time to diffuse away, the efficiency of the machining process is considerably higher. Very little debris was generated during the micromachining process, and what remains is not in the form of

hot droplets that attached to the surface; rather, the micromachining process by femtosecond laser pulses creates fine dusts that do not carry much heat, and therefore do not bind to the surface. Using powerful gas jets such as dry air,  $\text{N}_2$  gas and He gas one might considerably reduce the amount of debris created, or one can push the debris far away from the work zone before re-deposition.

Fig. 7 shows 3D profiles of U-groove analyzed with 3D Surface Profiling System (SNU Precision Co., SIS-2000). The roughness of the bottom surface on the U-groove is measured less than  $\pm 1 \mu\text{m}$ . These results confirm the highly precise alignment of the optical fibers and the PLC chip in optical splitter packaging.

## 2. Optical Splitter Packaging

Our optical splitter packaging technique is to insert and align directly the single mode optical fiber with a corresponding waveguide of the PLC chip with engraved U-grooves, which are directly formed by laser micromachine techniques [17,18]. This packaging technique does not require the use of optical fiber array blocks in the active alignment and difficult etch-

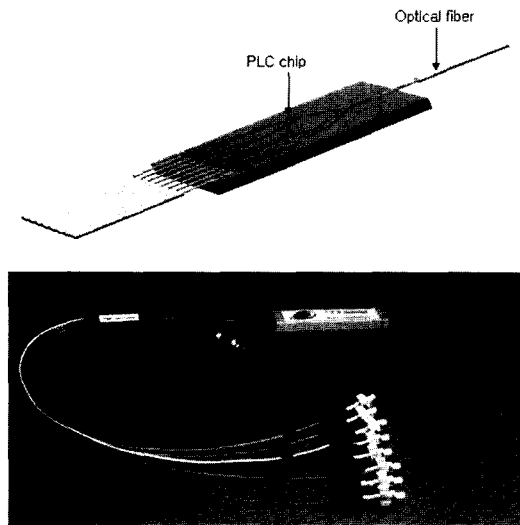


FIG. 8. A schematic and the product of  $1 \times 8$  PLC splitter module by the passive alignment packaging technique.

ing processes such as reactive ion etching through photolithography. It has advantages that substantially obviate one or more limitations and disadvantages of the conventional techniques, which involve considerable time and cost. Fig. 8 shows a schematic and the product of the  $1 \times 8$  PLC splitter module. This packaging technique can be applied for more functional hybrid PLC devices as well as PLC devices such as arrayed-waveguide gratings (AWG).

We measured optical characteristics of packaged  $1 \times 8$  PLC splitter modules, which are fabricated by the developed passive alignment technique without the fiber blocks. The insertion loss of three splitter modules was less than 11.0 dB at wavelength of  $1.55 \mu\text{m}$ . Typical loss spectra from 1300 nm to 1650 nm wavelength range of 8 channels were distributed within  $\pm 0.6$  dB, indicating that the WDL was small. The optical return loss from the interface between the fiber and the PLC chip was more than 55 dB at  $1.55 \mu\text{m}$ . The average PDL was also less than 0.2 dB at  $1.5 \mu\text{m}$ . These results confirm that the high accuracy tolerance of  $\pm 1 \mu\text{m}$  and the high stability of packaging technique in PLC are possible by femtosecond lasers.

## V. CONCLUSION

We have shown that it is possible to produce well-defined and highly reproducible U-grooves of  $126 \mu\text{m} \times 87 \mu\text{m} \times 2 \text{ mm}$  in PLC chip with a femtosecond laser system of 800 nm wavelength (Ti:Sapphire) and pulse lengths of 100 fs. On the other hand, the ablation with nanosecond laser pulses (i.e. excimer laser) is accompanied with thermal or mechanical damages

and molten materials. Shock waves generated by a nanosecond laser were also observed on the surface of silica material. Femtosecond pulse lasers are suited to precise micromachining applications in silica materials since they have precise controllable threshold energy and negligible thermal diffusion. The ablation process with femtosecond laser pulses generates no contamination to the surrounding material, no molten zone, no microcracks, no shock wave, no delamination, no recast layer, and no damage to adjacent structure in silica materials, compared to nanosecond lasers.

We also showed that it was possible to fabricate optical devices such as  $1 \times 8$  optical splitter module with the micromachining technique based on femtosecond laser pulses. The insertion loss and the optical return loss of packaged  $1 \times 8$  optical splitter modules were less than 11.0 dB and more than 55 dB, respectively. The WDL was distributed within  $\pm 0.6$  dB and the PDL was less than 0.2 dB. These results also mean that the packaging technique using the passive alignment is excellent and femtosecond-pulsed laser micromachining technique could provide a new PLC packaging technology.

## ACKNOWLEDGMENT

The author would like to thank all members of PHOCO company in Korea for their valuable discussions and their contributions to this work.

\*Corresponding author : toby@icu.ac.kr.

## REFERENCES

- [1] F. N. Goodall, R. A. Moody, and W. T. Welford, "Reduction photolithography by ablation at wavelength 193nm," *Optical communications*, vol. 57, pp. 227-229, 1986.
- [2] R. Srinivasan, "Ablation of polymers and biological tissue by ultraviolet lasers, Science," *Science*, vol. 234, pp. 559-565, 1986.
- [3] V. Oliveira, O. Conde, and R. Vilar, "UV Laser Micromachining of Ceramic Materials: Formation of Columnar Topographies," *Advanced engineering materials*, Vol. 3, No.1/2, pp.75-81, 2001.
- [4] B. N. Chichkov, C. Momma, S. Nolte, F. v. Alvensleben, and A. Tunnermann, "Femtosecond, picosecond and nanosecond laser ablation of solids," *Applied Physics A*, vol. 63, pp. 109-115, 1996.
- [5] C. Momma, B. N. Chichkov, S. Nolte, F. v. Alvensleben, A. Tunnermann, H. Welling, and B. Wellegehausen, "Short-pulse laser ablation of solid targets," *Optics communications*, vol. 129, pp. 134-142, 1996.

- [6] C. Momma, S. Nolte, B. N. Chichkov, F. V. Alvensleben, and A. Tunnermann, "Precise laser ablation with ultrashort pulses," *Applied surface science*, vol. 109/110, pp. 15-19, 1997.
- [7] F. Korte, S. Nolte, B. N. Chichkov, T. Bauer, G. Kamlage, T. Wagner, C. Fallnich, and H. Welling, "Far-field and near-field material processing with femtosecond laser pulses," *Applied physics A Materials science & processing*, Vol. 69, No. 7, pp. S7-S11, 1999.
- [8] H. Varel, D. Ashkenasi, A. Rosenfeld, and M. Wahmer, "Micromachining of quartz with ultrashort laser pulses," *Applied physics A*, vol. 65, pp. 367-373, 1997.
- [9] J. Krüger, W. Kautek, M. Lenzner, S. Sartania, C. Spielmann, and F. Krausz, "Laser micromachining of barium aluminium borosilicate glass with pulse durations between 20 fs and 3 ps," *Applied surface science*, vol. 127-129, pp. 892-898, 1998.
- [10] S. Preuss, A. Demchuk, and M. Stuke, "Sub-picosecond UV laser ablation of metals," *Applied physics*, vol. 61, pp 33-37, 1995.
- [11] Ameer-Beg, W. Perrie, S. Rathbone, J. Wright, and W. Weaver, "Femtosecond laser microstructuring of materials," *Applied surface science*, vol. 127-129, pp. 875-880, 1998.
- [12] M. Kawachi, "Recent progress in silica-based planar lightwave circuits on silicon," *IEE Proc.-Optoelectron.*, vol. 143, pp. 257-262, 1996.
- [13] S. I. Anisimov, M. I. Tribel'skii, and Ya.G. Epel'baum, *Sov. Phys., JETP* 51, pp. 802-807, 1980.
- [14] Y. Hibino, F. Hanawa, H. Nakagome, M. Ishi, and N. Takato, "High reliability optical splitters composed of silica-based planar lightwave circuits," *Journal of lightwave technology*, vol. 13, pp. 1728-1735, 1995.
- [15] A. Sugita, K. Onose, Y. Ohmori, and M. Yasu, "Optical fiber coupling to single-mode silica-based planar lightwaveguide circuits with fiber-guiding grooves," *Fiber and integrated optics*, vol. 12, pp. 347-354, 1993.
- [16] C. Buerhop, B. Blumenthal, R. Weissmann, N. Lutz, and S. Biermann, "Glass surface treatment with excimer and CO2 lasers," *Applied surface science*, vol. 46, pp. 430-434, 1990.
- [17] B. C. Choi, J. H. Choi, H. I. Lee, C. S. Park, and M. S. Lee, "The development of packaging technique in  $1 \times 8$  optical splitter using the passive alignment method," in *Proceedings of photonics conference '02*, pp. 703, 2002.
- [18] B. C. Choi, J. H. Choi, H. I. Lee, C. S. Park, and M. S. Lee, "The Passive alignment technique of fiber-to-waveguide," in *ICEP, '03*, pp. 122-126, 2003.